Charmed mesons have no discernible color-Coulomb attraction

T. Goldman* and Richard R. Silbar†
Theoretical Division, MS-B283, Los Alamos National Laboratory, Los Alamos, New Mexico 87545, USA
(Received 8 August 2011; published 19 January 2012)

Starting with a confining linear Lorentz scalar potential V_s and a Lorentz vector potential V_v, which is also linearly rising but has in addition a color-Coulomb attraction piece $-\alpha_s/r$, we solve the Dirac equation for the ground-state c- and u-quark wave functions. Then, convolving V_v with the u-quark density, we find that the Coulomb attraction almost completely washes out, making an essentially linear $\bar{V}_v$ for the c quark. A similar convolution using the c-quark density also leads to an essentially linear $\tilde{V}_v$ for the u quark. For bound $\bar{c}$-c charmonia, where one must solve using a reduced mass for the c quarks, we again find by convolution an essentially linear $\widehat{V}_v$. Thus, the relativistic quark model is consistent with the absence of a color-Coulomb attraction in the charmed-meson mass spectrum. To see if this near-linearity of V_v provides a reasonable model for the bound $\bar{c}$-c charmonium states, we then solve the radial Dirac equations for V_s and V_v, both with and without a color-Coulomb attraction at shorter distances. We present and compare the predictions of their masses for the two models. We find that a strictly linear V_v provides about as good a fit to the charmonia masses as the one with a color-Coulomb attraction, despite having one less parameter.

DOI: 10.1103/PhysRevC.85.015203 PACS number(s): 14.40.Lb, 12.39.−x, 14.40.Pq, 14.65.Dw

I. INTRODUCTION

By assuming mesons to be quark-antiquark bound states and using the so-called "Cornell potential" [1]

$$V_{\rm Cor}(r) = -C_F\frac{\alpha_s}{r} + \kappa^2 r, \tag{1}$$

nonrelativistic solutions of the Schrödinger equation have been remarkably successful in predicting features of the meson spectrum in terms of two parameters. Here $C_F = \frac{4}{3}$ is the color factor, $\alpha_s = {g_s}^2/4\pi$, with g_s being the (running) quark-gluon coupling constant, and κ is the string tension (in fm^{-1}). It is the linear term in $V_{\rm Cor}(r)$ that confines the quarks, similar to the confinement in the relativistic bag model. [2]

However, nonrelativistic potential models for *charmonium* states [3] have also done remarkably well at describing these states with a simple linear confining potential (plus spin-spin and spin-orbit terms), *absent* any evidence for a short distance color-Coulomb contribution. This finding is somewhat surprising as, early on, the high mass of the charm quark suggested that the color-Coulomb region might be discernible, at least in the wave functions, if not the eigenenergies. Here we find the effect to be negligible in the latter and not significant in the former, with a relativistic quantum mechanical approach to $\bar{c}$-c charmonium states using the Dirac equation.

For a relativistic model the two terms in $V_{\rm Cor}(r)$ have different Lorentz transformation properties. The color-Coulomb potential α_s/r is naturally the fourth component of a Lorentz vector, which we will take as a part of a Lorentz vector potential $V_v(r)$. On the other hand, relativistic linear confinement requires a Lorentz scalar, which we take as a scalar potential $V_s(r)$. (The q-q vector interaction is attractive or repulsive depending upon whether the two quarks are in a color $\bar{\mathbf{3}}$ or color $\mathbf{6}$ irrep and so cannot confine directly. The scalar interaction avoids the repulsive channel entirely.)

Explicitly, the coupled radial Dirac equations [4–6] we solve in this paper are, in dimensionless form,

$$\begin{aligned} g_l{}'(x) + \frac{k}{x}g_l(x) - (\tilde{E} - V_v(x) + V_s(x) + \tilde{m})\, f_{l'}(x) = 0, \\ f_{l'}{}'(x) - \frac{k}{x}f_{l'}(r) + (\tilde{E} - V_v(x) - V_s(r) - \tilde{m})\, g_l(x) = 0, \end{aligned} \tag{2}$$

where $x = \kappa r$ is a dimensionless distance and the dimensionless energy and mass are $\tilde{E} = E/\kappa$ and $\tilde{m} = m/\kappa$. Also, l and $l' = 2j - l$ are the orbital angular momenta for the upper component $g_l(x)$ and lower component $f_{l'}(x)$, respectively. The integer k is determined by the angular momentum quantum numbers according to

$$k = -(l+1), \quad \text{if } j = l + \tfrac{1}{2}; \quad k = l, \quad \text{if } j = l - \tfrac{1}{2}. \tag{3}$$

The upper Dirac component $\psi_a(x)$ is given (up to a phase) by $g_l(x)/x$ and the lower component $\psi_b(x)$ by $f_{l'}(x)/x$. For real potentials, the radial wave functions can be chosen to be real.

Note that the sign for $V_v(x)$ in Eqs. (2) is opposite to that of the energy $\tilde{E}$, the fourth component of the momentum four-vector, while that for V_s matches that for the (current) quark mass $\tilde{m}$, also a Lorentz scalar. We will choose the parameters of the $V_s(x)$ and $V_v(x)$ confining potentials to reproduce the bound charmonia masses.

The vector potential is assumed to also be linearly rising, with the same slope as $V_s(r)$. The reason for this is that there is evidence in the *baryonic* spectrum that the spin-orbit interaction is suppressed [7]. Page, Goldman, and Ginocchio (PGG) [8] have shown that this can be due to a cancellation between a scalar potential V_s and a vector potential V_v having the same linear slope at large distances.

*tgoldman@lanl.gov
†silbar@lanl.gov

We have shown elsewhere [6], numerically, that this cancellation does occur if the (dimensionless) forms of the potentials are

$$V_s(x) = x, \quad V_v(x) = x - x_v, \quad \text{with} \quad x = \kappa r. \tag{4}$$

Here we have chosen $V_s(0) = 0$ to satisfy chiral symmetry at short distances and the parameter $x_v > 0$ displaces V_v to lie below V_s. However, the addition of the color-Coulomb term to V_v,

$$V_{v,\,\text{Coul}}(x) = -\frac{\alpha_s}{x} + x - x_v, \tag{5}$$

would break the PGG cancellation. This breaking could be considered desirable, since there is evidence for a non-negligible spin-orbit interaction in the *mesonic* spectrum. For example, the $1P$ charmonium states χ_0 and χ_2 differ in their masses by 142 MeV [9].

We have checked that potentials such as $V_s(x) = x$ and $V_v(x)$ as in Eq. (5) produces a reasonable representation of the charmonium spectrum to within ≈15 MeV. The details of this calculation are given in Sec. III and those following.

In doing such a calculation for $V_v(x)$ with the color-Coulomb attraction, however, we encountered an argument that suggests that the Coulomb attraction has no significant effect (hence the title for this article). We find that an *iterative, self-consistency requirement* on these potentials leads to a vector potential that is virtually indistinguishable from linear over the full range of interest. How this happens is discussed in Sec. II.

So, the question comes down to whether a strictly linear $V_v(x)$ as in Eq. (4) can do as well in predicting the bound charmonia masses. We find that it does. Details of calculations and comparison of results with and without the Coulomb term are presented in Sec. III.

II. WHY THE COLOR-COULOMB TERM DISAPPEARS

A. Convolving the vector potential

To see why the Coulomb attraction might be ineffective, we begin by considering the relativistic approach to the hydrogen atom. The Dirac equation is used for a reduced mass electron in a potential determined by the total charge interior to the radial point under consideration. This approach has been studied intensively by, for example, Friar and Negele [10]. For us, however, the closest analogy is to the case of D mesons, with one light quark and a heavy charm quark in the analogous role to that of the proton in Hydrogen.

As the light-quark mass is negligible on the scale of interest (we neglect effects of electromagnetism), there is no discernible reduced mass effect to consider. Furthermore, in hydrogen, the charge distribution within the proton (or nucleus in more massive atoms) smears out the Coulomb divergence at zero separation. Here, the charm quark is the color-Coulomb source but has no intrinsic internal structure. However, unlike the electromagnetic case, the strong virtual emission and reabsorption of gluons produces significant fluctuations in the color source location; for a very massive quark these are not negligible even to leading order.

Our approach is to take, as a first approximation, the charge distribution (rms size) of the D meson as setting a relevant scale for these fluctuations in smearing the color-Coulomb divergence. Although it may not be precise, given that the rms size is comparable to the inverse of the QCD mass scale, we consider this to be a very reasonable starting point. We use this scale to modify smoothly the color-Coulomb potential with a quadratically flat "bottom" and with slope equal to that of the $-\alpha_s/r$ color-Coulomb potential at a matching point.

We thus convolve the light-quark wave function with the color-Coulomb potential in the manner of Friar and Negele [10] to define the potential that the charm quark is subject to in the presence of the light quark. Finally, to check for self-consistency, we convolve *this* charm-quark wave function with the color-Coulomb potential to observe its effect on the light quark. We find a consistent, almost precisely linear, effective vector potential radially extending out all the way to the region where linear confining potentials are necessary for consistency with data. We provide the details of how this happens in the next four sections.

For charmonium states we then repeat the convolution for the c quark in interaction with a $\bar{c}$ quark. Here reduced mass effects are no longer negligible. We find (Sec. II F) a very similar result and conclude that there is indeed a single, consistent, approximately linear color vector potential that reasonably describes all of these states. Thus, there is no remaining evidence of the color-Coulomb potential in the charmed mesons, despite the relatively large mass of the c quark.

B. The vector potential containing a color-Coulomb term

After some numerical experimentation we focused on the charmed D mesons $\bar{c}$-u and (bound) charmonia $\bar{c}$-c as resulting from scalar and vector potentials $V_s(x)$ and $V_v(x)$ such as those shown in Fig. 1. As stated earlier, these potentials are dimensionless functions of a dimensionless radial coordinate $x = \kappa r$, where κ^2 is about 1 GeV/fm [11]. The asymptotically linear slopes of V_s and V_v were taken to be the same, in accordance with the small spin-orbit splitting in the baryon spectrum [7,8].

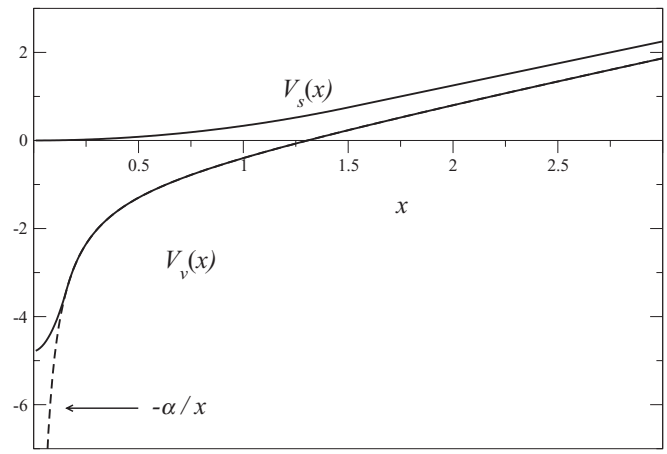

FIG. 1. The scalar and vector potentials $V_s(x)$ and $V_v(x)$ as functions of a dimensionless radial coordinate x.

The V_s is quadratic out to $x = 1.5$, after which it is strictly linear:

$$V_s(x) = \begin{cases} x^2/(2x_s) & \text{if } x < x_s, \\ x - x_s/2 & \text{otherwise,} \end{cases} \tag{6}$$

where the parameter x_s is, for us, fixed at 1.5. The flatness near $x = 0$ is to preserve chiral symmetry at short distances.

The V_v has, in addition to the linear confinement, a color-Coulomb contribution

$$V_v(x) = -C_F \frac{\alpha_s}{x} + x - x_v, \tag{7}$$

as shown by the dashed part in Fig. 1.

However, this is the potential seen by, say, the light u quark in the field of the heavy $\bar{c}$ quark, which is itself moving about somewhat in the field of the u quark. Thus, as discussed above, it is reasonable to moderate the singularity at $x = 0$. We did this simply by altering the potential to

$$V_{v,\,\mathrm{Coul}}(x) = \begin{cases} C_F\,\alpha_s\left(x^2 - 3x_D^2\right)/2x_D^3 + x - x_v & \text{if } x < x_D, \\ -C_F\,\alpha_s/x + x - x_v & \text{otherwise,} \end{cases} \tag{8}$$

assuming the smoothing to be about the size of the (electric) charge radius (R_D) of the $D(1869)$ meson. Here $x_D = 0.16$ is a reasonable guess (corresponding to $R_D \sim 0.3$ fm),

The plots in Fig. 1 are shown for the parameters α_s and x_v that give the best figures of merit we found for our fit (described in Sec. III and below) for charmonium states:

$$\begin{aligned} &\kappa^2 = 0.900\,\mathrm{GeV/fm}, \quad m_c = 1.567\,\mathrm{GeV}, \\ &x_v = 1.127, \quad \text{and} \quad \alpha_s = 0.3. \end{aligned} \tag{9}$$

The κ^2 in Eq. (9) for the color-Coulomb case is the same as that used in Ref. [11] and is consistent with that used in the Cornell potential, Eq. (1). For charmonia calculations, the mass in the coupled differential equations must be the reduced mass $m_c/2$. The masses we fit are those of the η_c, J/ψ, η_c', ψ', χ_0, and χ_2. [9]

We will also, in Sec. III, compare how well the above-mentioned fit with a color-Coulomb attraction compares with a $V_v(x)$ that is strictly linear, i.e.,

$$V_{v,\,\mathrm{linear}}\,(x) = x - x_v. \tag{10}$$

C. Convolving the Coulomb potential for the $\bar{c}$ quark

As mentioned above in Sec. II A, a more consistent way of moderating the Coulomb singularity is first to solve for the light u-quark $1s$ ground-state wave functions [6] for the potentials $V_s(x)$, Eq. (6), and V_v, Eq. (8), with $x_v = 1.127$ and $\alpha_s = 0.3$. The corresponding energy eigenvalue $E_u(1s) = 0.363$ GeV.

Given that u-quark wave function, the vector potential that the $\bar{c}$ quark should be subject to is the (unrounded) V_v given by Eq. (7) modulated by the density of that u quark. That is, following Friar and Negele's discussion of muonic atoms [10], the Coulomb potential should be convolved with the local "charge" density defined by the u-quark Dirac wave function. That, together with the linear contribution, gives a *new* vector potential for the $\bar{c}$ quark,

$$\bar{V}_v(x) = Q_{\mathrm{in}}(x)/x + Q_{\mathrm{out}}(x) + x - x_v, \tag{11}$$

where

$$\begin{aligned} Q_{\mathrm{in}}(x)/x &= -\frac{\alpha_s}{x}\int_0^x x'^2 dx'\ \psi^\dagger_{u,1s}(x')\psi_{u,1s}(x') \\ &= -\frac{\alpha_s}{x}\int_0^x x'^2 dx'\left[\psi_a^2(x') + \psi_b^2(x')\right], \\ Q_{\mathrm{out}}(x) &= -\alpha_s\int_x^\infty x'\,dx'\ \psi^\dagger_{u,1s}(x')\psi_{u,1s}(x') \\ &= -\alpha_s\int_x^\infty x'\,dx'\left[\psi_a^2(x') + \psi_b^2(x')\right]. \end{aligned} \tag{12}$$

Here $\psi_a(x)$ is the (real) upper Dirac component and $\psi_b(x)$ the lower component.

Near $x = 0$,

$$Q_{\mathrm{in}}(x)/x \approx \frac{|\psi(0)|^2}{x}\int_0^x x'^2 dx' = \frac{|\psi(0)|^2\,x^2}{3} \tag{13}$$

and it never gets more negative than about -0.2 before it increases again toward zero like $-\alpha_s/r$. As for $Q_{\mathrm{out}}(x)$, since the $1s$ upper-component radial wave function is well approximated as a Gaussian [11,12], its integral gives, approximately, $-\alpha_s$ times a (narrower) Gaussian.

A plot of $\bar{V}_v(x)$ calculated from the integrals of Eq. (12) is given in Fig. 2. Despite its appearance, it is not strictly a straight line: there is some small curvature in the plot below $x = 1$. Nonetheless, we consider the high accuracy of a linear approximation to be rather surprising, as we were expecting only a minor change in the effective value of x_D. The dashed line in Fig. 2 is a linear fit to $\bar{V}_v(x)$ with slope 1.1045 and displacement -1.5008.

D. How ψ_c changes with the new potential

If one solves for the $1s$ state of the $\bar{c}$ quark for $m_c = 1.567$ GeV and the original potentials of Eq. (6) and Eq. (8), one finds the $\bar{c}$-quark eigenenergy to be $E_c(1s) = 1.299$ GeV. That is, the energy of the c quark for these potentials is some 200 MeV less than its mass. The upper and lower $1s$ radial wave functions are displayed in Fig. 3 as dashed curves. The rise of ψ_a at the origin is reminiscent of the nonrelativistic ground-state wave function for a pure Coulomb potential,

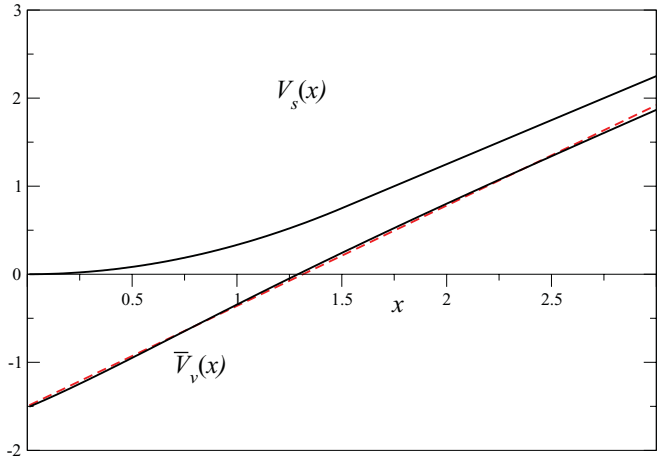

FIG. 2. (Color online) The scalar potential $V_s(x)$ and the convolved vector potential $\bar{V}_v(x)$ for the $\bar{c}$ quark as functions of x. The dashed curve (nearly overlying the solid line) is a linear fit to $\bar{V}_v(x)$.

which is a wave function that is a decaying exponential like $e^{-\alpha x}$.

However, solving for $E_c(1s)$ with $V_s(x)$ and the *convolved* $\bar{V}_v(x)$, we find $E_c(1s) = 1.538$ GeV, now considerably higher in energy because of the missing Coulomb well, although still a bit less than $m_c = 1.567$ GeV. The upper and lower component wave functions, shown as the solid curves in Fig. 3, are broader than those found for the original potentials. (In both cases, however, the $\bar{c}$-quark wave functions are not as broad as those for the u quark.)

Thus, while the mass of a $\bar{c}$-u D meson depends strongly on $E_c(1s)$, it is not very sensitive to the difference between the original and convolved potentials; the wave functions are quite different. We therefore expect that quantities such as transition strengths, which are more dependent on the details of the wave functions, will be more potential-dependent than the masses are.

E. Convolving for the u-quark potential

Continuing, we find that the singular Coulomb piece of the vector potential seen by the u quark is also smeared by

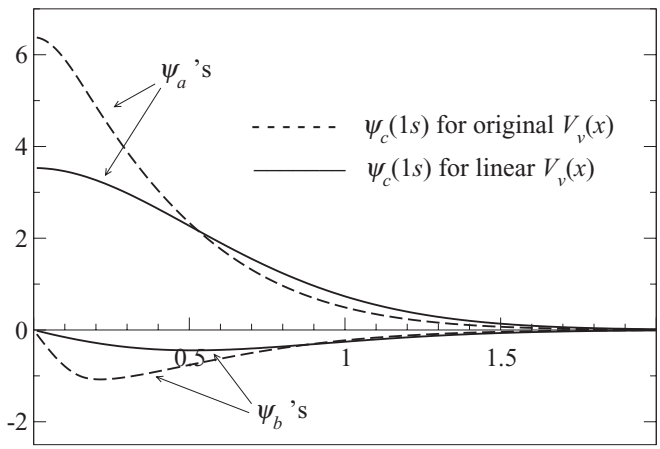

FIG. 3. Comparing the $\bar{c}$-quark radial wave functions for the original and convoluted potentials.

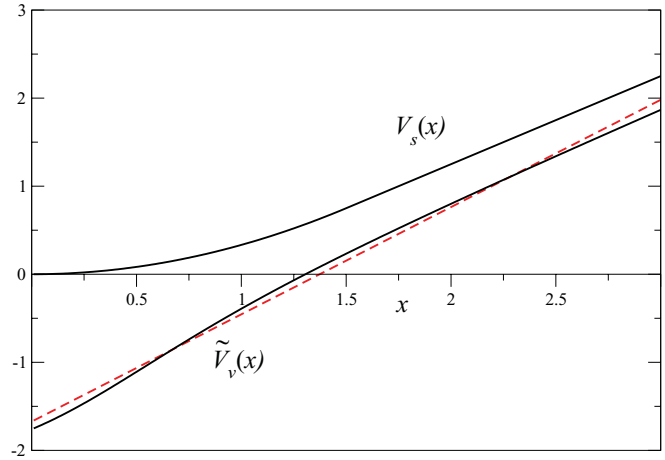

FIG. 4. (Color online) The scalar potential $V_s(x)$ and the convolved vector potential $\tilde{V}_v(x)$ for the u quark as functions of x. The dashed curve is a linear fit to $\tilde{V}_v(x)$.

the motion of the somewhat more confined, slower moving $\bar{c}$ quark. With formulas like Eqs. (11) and (12), but with the density provided by $|\psi_c(1s)|^2$, we again found this second convolution is also very close to linear, as shown in Fig. 4. In making this plot we used the $\psi_c(1s)$ found from using $\bar{V}_v$. Again, the dashed line is a linear fit to $\tilde{V}_v(x)$ with slope $a_0 = 1.167$ and displacement $a_1 = -1.640$.

The $\tilde{V}_v$ is slightly more curved and a bit deeper than the $\bar{V}_v$ shown in Fig. 2, but is essentially the same nearly linear potential as that which affects the $\bar{c}$ quark. Although the linear fit parameters are slightly different, in a strictly linear model one could reasonably assume the same linear potential for both quarks. We demonstrate this below.

F. Convolving for charmonium

Similarly, we investigated the smearing of the Coulomb potential for $\bar{c}$-c charmonia states. In this case we must solve using the reduced mass $m_c/2 = 0.784$ GeV, but otherwise the calculation proceeds much as above. First we find the wave functions for the c quark for the original potentials $V_s(x)$ [Eq. (6)] and V_v [Eq. (8)]. Then, convolving the singular Coulomb potential with $|\psi_{c,\,\text{reduced}}|^2$ as in Eqs. (11) and (12), we obtain the plot of $\widehat{V}_v$ shown in Fig. 5. The dashed line is a linear fit to $\widehat{V}_v(x)$ with slope $a_0 = 1.169$ and displacement $a_1 = -1.644$. Note that the linear fit parameters are quite close to the values that we found for the (effective) potential for the u quark.

III. CHARMONIA STATES, WITH AND WITHOUT A COULOMB TERM

A. Setting the quark masses

To proceed, we need to set the masses and find the relativistic wave functions for the quarks of interest in this paper, namely, q (standing for either u or d) and c. This involves solving Eqs. (2) for each (current quark) mass m to obtain the energy eigenvalues $E(nlj)$ for the different

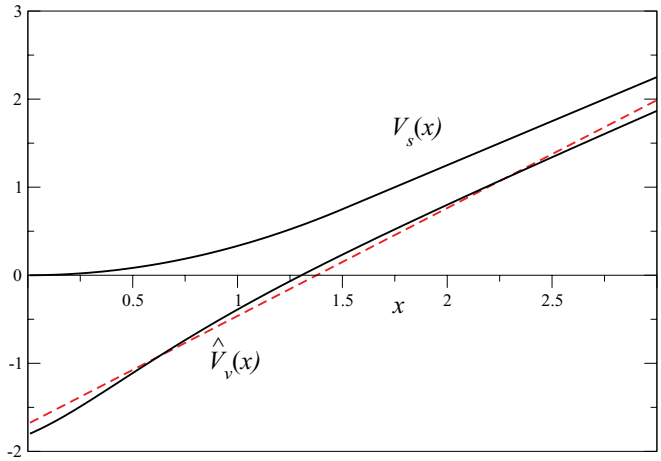

FIG. 5. (Color online) The scalar potential $V_s(x)$ and the convolved vector potential $\widehat{V}_v(x)$ for charmonia states as functions of x. The dashed curve is a linear fit to $\widehat{V}_v(x)$.

quarks and their respective upper and lower component wave functions. We do this using a "shoot and match" technique described in detail in Ref. [6].

First, we treat the q quarks, which we assume are both of negligible mass; that is, we set $m_q = 0$. It is because they are light compared to the inverse size-scale of hadrons that we consider it necessary to go to a relativistic version of the quark model of mesons. For the lowest bound q-$\bar{q}$ states, namely the π and ρ mesons, the $l = 0$, $j = \frac{1}{2}$ energy $E_q(1s)$ is roughly 0.310 GeV, which is frequently thought of as a "constituent mass" for the massless quark, as opposed to its "current" mass. In this paper, because of well known complications of glueballs, channel coupling, and the axial anomaly, we will not treat these and other q-$\bar{q}$ light mesons.

For the case of the linear $V_{v,\,\mathrm{linear}}(x)$, we note that the wave functions found from solving the Dirac ODEs of Eq. (2) are invariant with respect to the combination $\tilde{E} + x_v$. That is, $\tilde{E} + x_v$ is essentially the eigenvalue for the bound-state wave function. Thus, the desired $E_q(1s)$ is obtained by adjusting x_v to the value given in Eq. (16).

For fixing the charmed-quark mass, we can use the lightest $1S$ c-$\bar{q}$ mesons, $M_D(1869)$ and $M_{D^*}(2010)$. To do so, we invoke a hydrogen-atom-like approximation, with the heavy c quark acting as the proton,

$$\begin{aligned} M_D &= m_c + E_q - \langle T_q \rangle - 3E_{\mathrm{CMI}} \\ M_{D^*} &= m_c + E_q - \langle T_q \rangle + E_{\mathrm{CMI}}, \end{aligned} \tag{14}$$

where $\langle T_q \rangle$ is the kinetic energy of the light quark. This subtracted average corrects approximately for the motion of the center of mass of the hydrogen-atom-like state due to the motion of the light quark. The experimental, weighted average mass [9] of these $1S$ mesons is

$$\begin{aligned} \bar{M}_D(1S) &= (M_D + 3M_{D^*})/4 = 1.975\ \mathrm{GeV} \\ &= m_c + E_q(1s) - \frac{\langle p_q^2 \rangle}{2\bar{M}_D(1S)} \\ &= m_c + E_q(1s) - \frac{E_q{}^2(1s)}{2\bar{M}_D(1S)}, \end{aligned} \tag{15}$$

where we used our approximation that $m_q = 0$ in the last equation.

For the case with $V_{v,\,\mathrm{Coul}}$, using the parameters in Eq. (9), integrating the radial equations yields $E_q(1s) = 0.462$ GeV. This energy is larger than the value relevant to light q-$\bar{q}$ mesons, $\approx$0.310 GeV, which is to be expected since the q quark is here more tightly localized. Thus, from Eq. (15), $m_c = 1.567$ GeV. This m_c is larger than the Particle Data Group (PDG) value of about 1.250 GeV [13] but is not inconsistent, as that value is derived from data using a nonrelativistic approach.

For the (strictly) linear V_v case, we simply take m_c as one of two parameters to be fit, along with V_0. (We also *fixed* the value of x_v at 1.7, based on the near-linear $V_v(x)$'s found in Sec. II and on the discussion above regarding the invariance of the ODEs with regard to $\tilde{E} + x_v$.) The best-fit values we found are

$$m_c = 1.518\ \mathrm{GeV} \quad \text{and} \quad V_0 = 1.253\ \mathrm{GeV/fm}. \tag{16}$$

This charmed-quark mass is close to the value found from Eq. (15).

We can also use the splitting of the D and D^* meson masses to fix the sizes of the color-magnetic interactions, E_{CMI}, in Eq. (14) and later on for the charmonia states. To do this we only need to know the q- and c-quark $1s$ wave functions and how the color-magnetic interaction depends upon them, discussed next.

B. The color-magnetic interaction: the simple cases

A large part of the attractive interaction between two quarks (or a quark and an antiquark) comes from one-gluon exchange between them, a four-vector interaction. The induced, effective scalar part of that interaction is considered to be largely responsible for the linear confinement we invoked in Eq. (4). The three-vector part constitutes the color-magnetic (or hyperfine) interaction, whose matrix element, the interaction energy for quarks "1" and "2", is

$$\begin{aligned} M_{CM} = -\int d^3x_1 \int d^3x_2\ \psi_1^\dagger(\mathbf{x}_1)\ \boldsymbol{\alpha}\ \psi_1(\mathbf{x}_1) \\ \cdot \psi_2^\dagger(\mathbf{x}_2)\ \boldsymbol{\alpha}\ \psi_2(\mathbf{x}_2)\ G(\mathbf{x}_1, \mathbf{x}_2), \end{aligned} \tag{17}$$

where $\boldsymbol{\alpha}$ is the usual Dirac matrix and $G(\mathbf{x}_1, \mathbf{x}_2)$ is the gluon propagator, having dimensions of energy.

In this section we derive an expression for the simple cases of interest in this paper, where there is only one way of forming a c-$\bar{c}$ state with J^{PC} from the single quark values of l_1, j_1 and l_2, j_2. This allows us to calculate the masses of the following charmonium states: $\eta_c(J^{PC} = 0^{-+})$ at 2.980 GeV, $J/\psi(1^{--})$ at 3.097 GeV, $\eta_c{}'(0^{-+})$ at 3.637 GeV, $\psi'(1^{--})$ at 3.686 GeV, $\chi_0(0^{++})$ at 3.415 GeV, and $\chi_2(2^{++})$ at 3.556 GeV. More complicated cases (not considered here) in which some particular combination of l_1, j_1 and l_2, j_2 forms the state with J^{PC} are not treated here, but can be derived using techniques of Racah algebra [14].

For an s state, the Dirac wave function ψ simplifies to

$$\psi(\mathbf{r}) = \begin{bmatrix} \psi_a(r) \\ -i\boldsymbol{\sigma} \cdot \hat{\mathbf{r}}\ \psi_b(r) \end{bmatrix} Y_{00}\ \chi_{m_s}, \tag{18}$$

where χ is a two-component Pauli spinor carrying the the magnetic quantum number $m_s = \pm 1/2$.

One often takes $G(\mathbf{x}_1, \mathbf{x}_2)$ to be a Yukawa propagator for the massless gluon exchange, with a cutoff $e^{-\mu x}$ to model the shielding about the quarks. In this paper, however, we will use a Gaussian form for the propagator [11] that allows us to perform the angular integrations in Eq. (17) more easily,

$$G(\mathbf{x}_1, \mathbf{x}_2) = \lambda\, e^{-\mu(\mathbf{x_1}-\mathbf{x_1})^2}, \tag{19}$$

where the parameter μ is dimensionless and the parameter λ has dimensions of energy and is proportional to $(C_F\alpha_s)^2$. Since the actual spatial Green function is unknown, except for a finite range, there is no real preference for the choice of a phenomenological propagator.

It turns out that our model's predictions are quite insensitive to the value of μ, and we therefore choose it to be 0.8 (corresponding to a cutoff separation scale between the quarks of about 0.5 fm). As stated above, we will fix the value of the λ parameter from the mass splittings between the $D^*(2010)$ and $D(1869)$ mesons, then use that value of λ to predict splittings of the bound charmonium mass states ($1S$, $2S$, and $2P$).

After some algebra, we can reduce Eq. (17) to

$$M_{CM} = \tfrac{8}{3}\, C_F\, \lambda\, I(\mu)\, \langle \boldsymbol{\sigma_1}\cdot\boldsymbol{\sigma_2}\rangle = \tfrac{32}{9}\, \lambda\, I(\mu)\, \langle \boldsymbol{\sigma_1}\cdot\boldsymbol{\sigma_2}\rangle, \tag{20}$$

The factor $\langle \boldsymbol{\sigma_1}\cdot\boldsymbol{\sigma_2}\rangle$ is 1 for $S = 1$ states and -3 for $S = 0$ states. Here $I(\mu)$ is a dimensionless double integral over the radial wave functions of quarks "1" and "2",

$$I(\mu) = \frac{1}{2\mu^2}\int_0^\infty dx_1 \int_0^\infty dx_2\; \psi_{1,a}(x_1)\, \psi_{1,b}(x_1) \times \psi_{2,a}(x_2)\, \psi_{2,b}(x_2)\big\{(2\mu x_1 x_2 - 1)\, e^{-\mu(x_1-x_2)^2} + (2\mu x_1 x_2 + 1)\, e^{-\mu(x_1+x_2)^2}\big\}. \tag{21}$$

Using the radial wave functions found by solving the coupled ODEs for the parameters of Eq. (9), we evaluate this double integral using $c(1s)$ and $\bar{q}(1s)$ ground-state wave functions to find $I(\mu = 0.8)$, getting

$$I_{c(1s),\,q(1s)} = \begin{cases} 0.0896 & \text{for } V_{v,\,\text{Coul}}\,(x), \\ 0.0736 & \text{for } V_{v,\,\text{linear}}\,(x), \end{cases} \tag{22}$$

the difference here reflecting the differences in the wave functions.

We can now determine the color-magnetic energy scale from the $1S$ D^*-D experimental mass difference,

$$E_{\text{CMI}} \equiv M_{CM} = (M_{D^*} - M_D)/4 = 35.3\ \text{MeV}. \tag{23}$$

From $I_{c(1s),q(1s)}$, E_{CMI}, and Eq. (20), we find the Gaussian energy parameter in Eq. (19) to be

$$\lambda = \begin{cases} 0.111\text{GeV} & \text{for } V_{v,\,\text{Coul}}\,(x), \\ 0.134\text{GeV} & \text{for } V_{v,\,\text{linear}}\,(x). \end{cases} \tag{24}$$

We will assume that these values of λ are also valid for the charmonia states c-$\bar{c}$, since λ is proportional to α_s and thus λ ought not be much different at these two different energies.

C. The masses of the $1S$ states, η_c and J/ψ

Using the $m_c = 1.567$ GeV from Sec. III A, we can now proceed to calculate the various bound $c\,\bar{c}$ charmonium states. In these calculations, because of the equal masses of the two c quarks, we must use the *reduced* mass $m_c/2$; when we solve the ODEs of Eq. (2) to get the energy and wave functions of the ground-state c quark. We find, for the parameters of Eqs. (9) and (16),

$$E_{c,\,\text{red}}(1s) = \begin{cases} 0.718\text{GeV} & \text{for } V_{v,\,\text{Coul}}\,(x), \\ 0.790\text{GeV} & \text{for } V_{v,\,\text{linear}}\,(x). \end{cases} \tag{25}$$

The $1s$ wave functions for the reduced-mass c quark are displayed in Fig. 6 for both cases. These wave functions are not as peaked as those displayed in Fig. 3.

We first check the experimental value of the spin-averaged mass of the two $1S$ states,

$$\bar{M}_{\text{exp}}(1S) = \left(M_{\eta_c} + 3M_{J/\psi}\right)/\,4 = 3.068\ \text{GeV}. \tag{26}$$

In analogy to the hydrogen atom, the *calculated* value of the $\bar{M}(1S)$ average is

$$\bar{M}_{\text{calc}}(1S) = 2m_c + E_B(1s), \tag{27}$$

where the bound c-quark binding energy is

$$E_B(1s) = E_{c,\,\text{red}}(1s) - m_c/2. \tag{28}$$

From the above calculations, i.e., Eq. (25), we find

$$\bar{M}_{\text{calc}}(1S) = \begin{cases} 3.068\text{GeV} & \text{for } V_{v,\,\text{Coul}}\,(x), \\ 3.067\text{GeV} & \text{for } V_{v,\,\text{linear}}\,(x), \end{cases} \tag{29}$$

both very close to the experimental value.

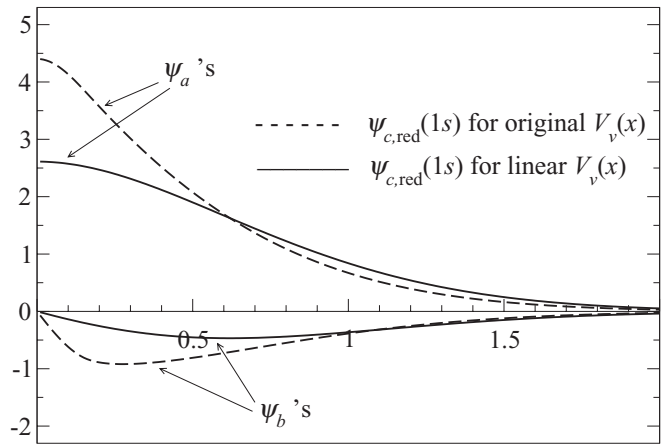

FIG. 6. Comparing the (normalized) reduced-mass c-quark $1s$ Dirac wave functions $\psi_{a,b}(x)$ for the two cases $V_{v,\,\text{Coul}}\,(x)$ (solid curve) and $V_{v,\,\text{linear}}\,(x)$ (dashed curve), for the parameters given in Eqs. (9) and (16).

TABLE I. Comparing results for the $1S$ and $2S$ bound charmonium states for the color-Coulomb and linear vector potentials.

$1S$ states				$2S$ states			
Quantity	$V_{v,\,\mathrm{Coul}}$	$V_{v,\,\mathrm{linear}}$	Experiment	Quantity	$V_{v,\,\mathrm{Coul}}$	$V_{v,\,\mathrm{linear}}$	Experiment
$E_{c,\,\mathrm{red}}(1s)$	0.718	0.790	–	$E_{c,\,\mathrm{red}}(2s)$	1.297	1.423	–
$E_B(1s)$	−0.066	0.031	–	$E_B(2s)$	0.513	0.664	–
$\bar{M}(1S)$	3.068	3.067	3.068	$\bar{M}(2S)$	3.647	3.700	3.674
$I_{c(1s),\,c(1s)}$	0.1013	0.0891	–	$I_{c(2s),\,c(1s)}$	0.0375	0.0336	–
M_{η_c}	2.984	2.940	2.980	$M_{\eta_c{}'}$	3.603	3.652	3.637
$M_{J/\psi}$	3.108	3.110	3.097	$M_{\psi'}$	3.662	3.716	3.686

To calculate the $1S$ mass splitting due to the color-magnetic interaction we use the reduced-mass c-quark radial wave functions (displayed in Fig. 6) in Eq. (21), obtaining

$$I_{c(1s),\,c(1s)} = \begin{cases} 0.1013 & \text{for } V_{v,\,\mathrm{Coul}}(x), \\ 0.0891 & \text{for } V_{v,\,\mathrm{linear}}(x). \end{cases} \tag{30}$$

With these values we find from Eq. (20), using the D-D^* value for lambda, Eq. (24),

$$\begin{aligned} M_{\eta_c} &= 2m_c + E_B(1s) - 3\,\tfrac{32}{9}\,\lambda\, I_{c(1s),\,c(1s)} \\ &= \begin{cases} 2.948\mathrm{GeV} & \text{for } V_{v,\,\mathrm{Coul}}(x), \\ 2.940\mathrm{GeV} & \text{for } V_{v,\,\mathrm{linear}}(x), \end{cases} \end{aligned} \tag{31}$$

$$\begin{aligned} M_{J/\psi} &= 2m_c + E_B(1s) + \tfrac{32}{9}\,\lambda\, I_{c(1s),\,c(1s)} \\ &= \begin{cases} 3.108\mathrm{GeV} & \text{for } V_{v,\,\mathrm{Coul}}(x), \\ 3.110\mathrm{GeV} & \text{for } V_{v,\,\mathrm{linear}}(x). \end{cases} \end{aligned} \tag{32}$$

The splitting between these states is a bit larger than the experimental splitting. Refinements for this splitting are discussed in Sec. III F.

D. The $2S$ States

To predict the excited $2S$ states, $\eta_c{}'$ at 3.637 GeV and ψ' at 3.686 GeV (which are still bound with respect to D-$\bar{D}$ decay), we need the (reduced mass) energy for the c quark in its excited $2s$ state. We solve the ODEs again for $l = 0$, $j = \frac{1}{2}$ and the potentials having the parameters of Eqs. (9) and (16), but this time with a higher trial energy. The wave functions ψ_a and ψ_b found for this excited state, not shown here, have the expected shapes [6] with one and two nodes, respectively. Again, those for the color-Coulomb case are narrower than those for the linear case.

Following the equations given in the previous subsection, we compare the calculated quantities and masses for the $1S$ and $2S$ states in Table I.

Despite $\bar{M}(2S)$ being fit in the iterations by fixing the parameters for the linear potential, it comes out about 30 MeV high compared with experiment. On the other hand, the Coulomb case finds $\bar{M}(2S)$ to be a bit low by the same amount. Also, the predicted splitting between J/ψ and η_c is larger than the experimental splitting, and it is more so for the linear case. Likewise, the ψ'-$\eta_c{}'$ splitting, $\approx$60 MeV, is more than the experimental 49 MeV. We discuss a possible refinement to the splittings for these states in Sec. III F.

E. The $1P$ states

There are four $1P$ states [9], but we will only predict the two that are simplest to evaluate, χ_0 at 3.415 GeV and χ_2 at 3.556 GeV. The two $J = 1$ states, χ_0 ($^3P_1$) and h_c ($^1P_1$), lie between them with nearly equal masses, and therefore they will mix with each other in an involved way, in contrast to the unmixed $^3P_0$ and $^3P_2$ states.

We model the χ_0 meson as a $c(2p\,\frac{1}{2})\,\bar{c}(1s\,\frac{1}{2})$ state with $J = 0$, $L = 1$, and $S = 1$. We need to solve the (reduced-mass) ODEs of Eq. (2) (with appropriately changed boundary conditions) for the $2p\,\frac{1}{2}$ excited state, which enters into the calculation of M_{χ_0}. We do likewise for χ_2, a $c(2p\,\frac{3}{2})\,\bar{c}(1s\,\frac{1}{2})$ state with $J = 2$, $L = 1$, and $S = 1$.

The energies $E_{c,\mathrm{red}}(2p\,\frac{1}{2})$ and $E_{c,\mathrm{red}}(2p\,\frac{3}{2})$ are about 250 MeV lower than $E_{c,\mathrm{red}}(2s)$. Plots of the upper and lower wave functions are as expected [6], again with the color-Coulomb wave functions narrower than the linear ones. For p-wave states, we expect the color-magnetic interaction to be small, as the hyperfine interaction (mostly) only affects s-wave states.

TABLE II. Comparing results for the $1P$ bound charmonium states, for the color-Coulomb and linear vector potentials.

Quantity	$\chi_0,\ nlj = \{2, 1, \frac{1}{2}\}$			$\chi_2,\ nlj = \{2, 1, \frac{3}{2}\}$		
	$V_{v,\,\mathrm{Coul}}$	$V_{v,\,\mathrm{linear}}$	Experiment	$V_{v,\,\mathrm{Coul}}$	$V_{v,\,\mathrm{linear}}$	Experiment
$E_{c,\,\mathrm{red}}(nlj)$	1.068	1.138	–	1.132	1.158	–
$E_B(nlj)$	0.284	0.379	–	0.348	0.399	–
$I_{c(2p),c(1s)}$	−0.0505	−0.0517	–	0.1065	0.0957	–
M_{χ_J}	3.399	3.390	3.415	3.524	3.481	3.556

We display the numerical results for the color-Coulomb and linear cases in Table II. The splitting between these two $1P$ states is about 125 MeV in the Coulomb case and 91 MeV the linear case, both of which are less than the experimental 141 MeV.

F. Can one improve the mass splittings?

As noted above, the predicted $1S$ and $2S$ mass splittings are somewhat larger than experiment. A somewhat smaller λ, and thus smaller mass splittings, would be found if we use the η_c-J/ψ splitting instead of the D^*-D mass splitting. From the c-quark wave functions we evaluate $I(c_{\rm red}1s, c_{\rm red}1s)$ and find

$$\lambda = \begin{cases} 0.078\text{GeV} & \text{for } V_{v,\,\text{Coul}}\,(x), \\ 0.104\text{GeV} & \text{for } V_{v,\,\text{linear}}\,(x). \end{cases} \tag{33}$$

to be compared with the values in Eq. (24).

IV. CONCLUSIONS

These results are consistent with the good spectral results found in nonrelativistic and relativistic models for the charmonium spectrum using linear confining potentials. It is unclear whether the slight differences in the effective linear potentials merit the complications of a relativistic approach to the calculation of spectra until high accuracies become necessary. Our convolution approach suggests that the good spectral results with a nonrelativistic, linear potential are due to the still relatively light mass of the charm quark. This in turn invites the question as to whether this status can still hold for the bottom quark. Absent detailed comparisons with transition rates for charmonium and D-meson decays, which one expects to be more sensitive to wave function details than are spectra, the color-Coulomb contribution to the effective potential for quark binding remains undetermined from charmonium mass data alone. We intend to turn next to bottom-quark states to examine whether the spectra there can provide a definitive determination of this issue.

ACKNOWLEDGMENTS

We thank James Friar for an illuminating conversation which led us to the convolutions in Eq. (12). This work was carried out in part under the auspices of the National Nuclear Security Administration of the US Department of Energy at Los Alamos National Laboratory, under Contract No. DE-AC52-06NA25396.

[1] E. Eichten, K. Gottfried, T. Kinoshita, J. Kogut, K. D. Lane, and T. M. Yan, Phys. Rev. Lett. **34**, 369 (1975); E. Eichten, K. Gottfried, T. Kinoshita, K. D. Lane, and T. M. Yan, Phys. Rev. D **17**, 3090 (1978); **21**, 203 (1980).

[2] C. E. DeTar and J. F. Donoghue, Annu. Rev. Nucl. Part. Sci. **33**, 235 (1983).

[3] See, e.g., C. Quigg and J. L. Rosner, Phys. Rep. **56**, 167 (1979). A more recent viewpoint of quarkonia by Rosner is available as arXiv:1107.1273 (2011).

[4] H. A. Bethe and E. E. Salpeter, *Quantum Mechanics of One- and Two-Electron Atoms* (Springer, Berlin, 1957), Sec. 14.

[5] J. D. Bjorken and S. D. Drell, *Relativistic Quantum Mechanics* (McGraw-Hill, New York, 1964), p. 55.

[6] R. R. Silbar and T. Goldman, Eur. J. Phys. **32**, 217 (2011).

[7] N. Isgur, Phys. Rev. D **62**, 054026 (2000); **62**, 014025 (2000).

[8] P. R. Page, T. Goldman, and J. N. Ginocchio, Phys. Rev. Lett. **86**, 204 (2001).

[9] The meson's masses and their other properties are compiled in C. Amsler *et al.* (Particle Data Group), Phys. Lett. B **667**, 586 (2008). A convenient access to this data is to go online to [http://pdglive.lbl.gov] and select the interactive listings.

[10] J. L. Friar and J. W. Negele, Phys. Lett. B **46**, 5 (1973).

[11] T. Goldman, K. R. Maltman, G. J. Stephenson Jr., and K. E. Schmidt, Nucl. Phys. A **481**, 621 (1988). This reference is henceforth abbreviated as GMSS.

[12] C. Critchfield, Phys. Rev. D **12**, 923 (1975).

[13] K. Nakamura *et al.* (Particle Data Group), J. Phys. G **37**, 075021 (2010). See [http://pdg.lbl.gov/2011/reviews/rpp2011-rev-quark-masses.pdf], p. 15, Fig. 3

[14] R. R. Silbar (unpublished); details can be provided to anyone who is interested.